

# FAMILIES OF SYMMETRIC-PERIODIC ORBITS IN THE ELLIPTIC THREE-DIMENSIONAL RESTRICTED THREE-BODY PROBLEM

E. SARRIS

*National Observatory of Athens, Astronomical Institute, Athens, Greece*

(Received 14 April, 1989)

**Abstract.** With an orbit of the three-dimensional circular problem as a starting point, we have calculated families of symmetric-periodic orbits in the three-dimensional elliptic problem with a variation of the mass ratio  $\mu$  and the eccentricity  $e$ . Afterwards, we have studied their evolution and stability.

## 1. Introduction

It is well known that, in the circular problem of three bodies, we can have periodic orbits with any value of the semi-period  $T$ . Thus, we can have the meaning of the family, in the space of the initial conditions, as a function of the period. This, however, cannot take place in the elliptic problem because the period can only be a multiple integer of  $2\pi$ . In the case of the elliptic problem we can have the meaning of the family by taking as a parameter the eccentricity  $e$ , or the mass ratio  $\mu$  of the primaries, in the space of the initial conditions.

Furthermore, it is also known that the elliptic periodic orbits approach the real motions of the celestial bodies more closely than the circular ones. For this reason, and also because the circular orbits have been extensively studied, we decided to study the evolution and behaviour of a circular orbit with a period  $2\pi$ , in the phase space  $(x, y, z, \dot{x}, \dot{y}, \dot{z})$ , introducing the eccentricity of the primaries, changing it, as well as changing the mass ratio. Thus, with the previous members of the family we decided to create families of periodic orbits, and at the same time study their stability.

The present study deals with the numerical investigation of the periodic orbits of the three-dimensional elliptic problem. This is achieved by extending the known periodic orbits of the circular problem.

Of previous investigators of this and similar subjects, Hunter (1967) investigated the motions of the satellites of Jupiter and of the asteroids in the Sun–Jupiter system. The orbits of the satellites are taken to be examples of the elliptical restricted, three-dimensional, three-body problem. Broucke (1969) has worked systematically on the plane-elliptic restricted three-body problem and he has found many families of periodic orbits and their stability. Finally, Katsiaris (1972) and Macris *et al.* (1975) have given some periodic-symmetric solutions of the three-dimensional elliptic orbits and their stability.

We use the equations of motion in the vibrating and rotating coordinate system (Kopal and Lyttleton, 1963), and we take the true anomaly  $v$  as an independent variable.

Hence, we set

$$\begin{aligned} \frac{dx_1}{dv} = x_4 = f_1, \quad \frac{dx_2}{dv} = x_5 = f_2, \quad \frac{dx_3}{dv} = x_6 = f_3, \\ \frac{dx_4}{dv} = 2x_5 + \frac{r}{p} \frac{\partial U}{\partial x_1} = f_4, \quad \frac{dx_5}{dv} = -2x_4 + \frac{r}{p} \frac{\partial U}{\partial x_2} = f_5, \\ \frac{dx_6}{dv} = -x_3 + \frac{\partial U}{\partial x_3} = f_6, \end{aligned} \quad (1)$$

where  $x_1, x_2, x_3$  are the coordinates and  $x_4, x_5, x_6$  the corresponding momenta. Also the potential function is defined as

$$U = (1 - \mu) \left( \frac{1}{r_1} + \frac{r_1^2}{2} \right) + \mu \left( \frac{1}{r_2} + \frac{r_2^2}{2} \right), \quad (2)$$

where

$$\begin{aligned} r_1^2 = (x_1 + \mu)^2 + x_2^2 + x_3^2, \quad r_2^2 = (x_1 + \mu - 1)^2 + x_2^2 + x_3^2, \quad p = 1 - e^2, \\ \mu = \frac{m_2}{m_1 + m_2}, \quad r = \frac{1 - e^2}{1 + e \cos v} \end{aligned}$$

and  $m_1, m_2$  the masses of the primaries.

## 2. The Symmetric-Periodic Orbits

By use of Equations (1) and the potential function (2), we can see immediately that if there are any symmetrical-periodic orbits then the coordinates of two symmetrical points from these orbits will be equal to or opposite, according to the symmetry.

The function  $U$  is of the form  $U = U(x_1, x_2^2, x_3^2)$ . Therefore, it will be symmetric with respect to the  $Ox_1$ -axis and to the  $Ox_1x_2$ -plane and  $Ox_1x_3$ -plane.

By starting with the circular problem at the times  $t$  and  $-t$  it follows that

$$\left. \begin{aligned} x_i(t) &= x_i(-t), \quad i = 1, 5, 6, \\ x_i(t) &= -x_i(-t), \quad i = 2, 3, 4. \end{aligned} \right\} \quad (3)$$

As we can observe from Equations (1) (where  $v = t$ ), the differentials of  $x_1 \dots x_6$  are symmetric. Therefore, the relations (3) are maintained throughout the whole orbit. This means that the orbit is symmetric with respect to the  $Ox_1$ -axis.

The relations (4) and (5) present symmetry with respect to the  $Ox_1x_3$ -plane ( $T =$  half-period): namely,

$$\left. \begin{aligned} x_i(t) &= x_i(T - t), \\ x_j(t) &= -x_j(T - t), \end{aligned} \right\} \quad i = 1, 3, 5, \quad j = 2, 4, 6, \quad (4)$$

$$\left. \begin{aligned} x_i(t) &= x_i(-t), \\ x_j(t) &= -x_j(-t), \end{aligned} \right\} \quad j = 2, 4, 6, \quad i = 1, 3, 5, \quad (5)$$

In the same way, the relations (6) are symmetric with respect to the  $Ox_1x_2$ -plane: namely,

$$\left. \begin{aligned} x_i(t) &= x_i(T + t), \quad i = 1, 2, 4, 5, \\ x_j(t) &= -x_j(T + t), \quad j = 3, 6. \end{aligned} \right\} \quad (6)$$

If now the third body start with initial conditions  $X_{0j} \neq 0$  ( $j = 1, 5, 6$ ) and  $x_{0j} = 0$  ( $j = 2, 3, 4$ ) (that is perpendicularly to the  $Ox_1$ -axis) and intersects the same axis perpendicularly again at time  $T$ , then, because of the symmetry, the orbit will pass from the same starting point at time  $2T$  and with the same initial conditions. Therefore, the orbit will be periodic.

The same it will be happen if we have symmetry with respect to  $Ox_1x_3$  or  $Ox_1x_2$  planes. For example, if the third body starts with initial conditions  $x_{0j} = 0$  ( $j = 2, 4, 6$ ) (i.e., perpendicularly to the  $Ox_1x_3$ -plane), and intersects the same plane again perpendicularly in time  $T$ , then, because of the symmetry, the orbit will pass from the same starting point at time  $2T$  and with the same initial conditions.

Equations (3) mean that the solutions are symmetric with respect to the  $Ox_1$ -axis, whereas Equations (4), (5), and (6) are symmetric with respect to the  $Ox_1x_3$  and  $Ox_1x_2$  planes, respectively.

We note that Equations (3) and (4) may both be valid at the same time. Therefore, the solution is symmetric with respect to the  $Ox_1$ -axis and the  $Ox_1x_3$ -plane, simultaneously. The same it happens at the relations (3) and (6). Therefore, the solution is simultaneously symmetric with respect to the  $Ox_1$ -axis and the  $Ox_1x_2$ -plane. Similarly to the previous, the relations (3), (4), and (6) can all be valid at the same time. This means that the solution is symmetrical simultaneously with respect to the  $Ox_1$ -axis, the  $Ox_1x_3$ - and  $Ox_1x_2$ -planes.

Now, we are able to examine what can happen in the elliptic problem.

In this case we can see from Equation (1) that instead of the time  $t$  we have the true anomaly  $v$ , as well as the factor  $r = (1 - e^2)/(1 + e \cos v)$ . Furthermore, the period  $2T$  can only take the values  $2k\pi$  ( $k = \text{integer}$ ). Thus, in order to have symmetry, the factor  $r$  must take the same value for two different values of  $v$ . This can happen only when the independent variable  $v$  takes the values  $\pi - v$  and  $\pi + v$  or  $v$  and  $-v$ .

Hence, the only requirement is to satisfy Equations (3) and (5). If the condition  $x_{0j} = 0$  ( $j = 2, 3, 4$ ) is valid, then we shall have symmetry with respect to the  $Ox_1$ -axis; whereas if the condition  $x_{0j} = 0$  ( $j = 2, 4, 6$ ) is valid, we shall have symmetry with respect to the  $Ox_1x_3$ -plane.

As it is easy to see, Equations (3) and (5) cannot be simultaneously satisfied. Therefore, in the elliptic problem we cannot have axial and bilateral symmetry at the same time.

### 3. Stability

The study of the stability of the solution was made through the eigenvalues of the Jacobian.

$$\Delta = (\bar{x}_0, v_0, 2T) = \left( \frac{\partial \bar{x}_i}{\partial x_{0j}} \right) \quad i, j = 1, 2, \dots, 6, \quad (7)$$

where  $\bar{x}_0$  is the initial position vector,  $T$  the half-period  $v_0 = 0$  or  $v_0 = \pi$ , and  $\bar{x}_i$  the position vector of the third body.

The characteristic equation of  $\Delta$  is of the form

$$|\Delta(\bar{x}_0, v_0, 2T) - \lambda I| = 0, \quad (8)$$

where  $I$  is the identity matrix of the sixth order.

Equation (8) takes the form

$$\lambda^6 + \alpha_1 \lambda^5 + \alpha_2 \lambda^4 + \alpha_3 \lambda^3 + \alpha_2 \lambda^2 + \alpha_1 \lambda + 1 = 0, \quad (9)$$

and its roots are  $\lambda_1, \lambda_2, \lambda_3$  and  $\lambda_1^{-1}, \lambda_2^{-1}, \lambda_3^{-1}$ . If we set

$$-k_1 = \lambda_1 + \frac{1}{\lambda_1}, \quad -k_2 = \lambda_2 + \frac{1}{\lambda_2}, \quad -k_3 = \lambda_3 + \frac{1}{\lambda_3},$$

we find that

$$k^3 - \alpha_1 k^2 + (\alpha_2 - 3) + (\alpha_3 - 2\alpha_1) = 0;$$

and if so,

$$Z^3 - 3qZ - 2r = 0, \quad (10)$$

where we have put

$$Z = k - \frac{\alpha_1}{3}, \quad q = \frac{1}{3}\alpha_2 - \frac{\alpha_1^2}{9}, \quad \text{and} \quad r = \frac{1}{2}(\alpha_3 - \alpha_1) - \frac{1}{6}\alpha_1\alpha_2 + \frac{\alpha_1^3}{27}.$$

In view of Equation (10) it follows that:

(1) If  $q^3 + r^2 > 0$ , then the solutions will be always unstable.

(2) If  $q^3 + r^2 < 0$  and  $|Ki| \leq 2$  ( $i = 1, 2, 3$ ), then will have stable solutions only.

The stability coefficients  $\alpha_1, \alpha_2, \alpha_3$  of the characteristic Equation (8) define a three-dimensional space, which it can be divided into twelve regions by the surface: i.e.,

$$q^3 + r^3 = 0; \quad (11a)$$

$$k_i^2 - 4, \quad i = 1, 2, 3. \quad (11b)$$

The analytic form of Equation (11a) is

$$4\alpha_2^3 - \alpha_1^2\alpha_2^2 - 9\alpha_1^2 + 42\alpha_1^2\alpha_2 - 8\alpha_1^4 + 108\alpha_2 - 108 - 36\alpha_2^2 + \\ + 27\alpha_3^2 - 18\alpha_1\alpha_2\alpha_3 - 54\alpha_1\alpha_3 + \alpha_1^3\alpha_3 = 0. \quad (12)$$

Equation (12) describes a surface which is symmetric with respect to the  $\alpha_2$ -axis; the  $\alpha_3$ -axis has no common point. The origin of the axes belongs at the stability region.

The relations (11b) are given analytically by

$$\alpha_3 + 2\alpha_1 = \pm (2\alpha_2 + 2). \tag{13}$$

Equations (13) describe two planes symmetric with respects to the  $\alpha_2$ -axis.

Figure 13 shows the intersections of the surface (12) and the planes (13) by the plane  $OXY$ . Thus, the curves  $c$  and  $d$  represent the intersections of the surface (12) by the plane  $OXY$  and are symmetric with respect to the origin of the axes. The straight line  $a$  represents intersection of the surface  $\alpha_3 + 2\alpha_1 = 2\alpha_2 + 2$  and the straight line  $b$  the intersection of the surface  $\alpha_3 + 2\alpha_1 = -(2\alpha_2 + 2)$  by the plane  $OXY$ .

In Figure 13 we can see some of the twelve stability-instability regions. The regions 2, 6, 10, 11, 12 are not visible as these are totally out of the plane  $OXY$ , towards the negative half-space. Figure 14 shows the intersection of the surface (12) and of planes (13) by the plane  $OXZ$ . In Figure 14 only the regions 5 and 9 are not visible. The whole region 5 is out of the  $OYZ$ -plane and towards the negative half-space. The whole region 9 is out of the  $OYZ$ -plane and towards the positive half-space.

From the 12 regions only the No. 1 is stable.

#### 4. Numerical Results

As a starting point for the calculation we have taken the orbit with initial conditions (Bray and Goudas, 1966): namely,  $\bar{x}_0 = \bar{x}(x_{01}, \dots, x_{06})$  is the initial vector, with

$$\begin{aligned} x_{01} &= 1.12560589, & x_{02} &= x_{03} = x_{04} = 0, & x_{05} &= -1.58086, \\ x_{06} &= 0.894431, & \mu &= 0.4, & e &= 0.0 \quad \text{and} \quad 2T = 6.37092, \end{aligned}$$

where  $T$  is the half-period of the orbit. From this orbit we have found the orbit with the elements

$$\begin{aligned} x_{01} &= 1.1256, & x_{02} &= x_{03} = x_{04} = 0, & x_0 &= -1.5229, \\ x_{06} &= 0.9179, & \mu &= 0.4, & e &= 0.0, & 2T &= 2\pi. \end{aligned}$$

This orbit is the starting point of the calculation of all the families. The precise conditions of all the calculations was

$$x_2 \leq 10^{-7} \quad \text{and} \quad \sqrt{x_3^2 + x_4^2} \leq 10^{-6}.$$

The calculated families in the present study were classified in two groups. The first of them, in includes eleven families of periodic orbits, which they were found by changing the mass ratio  $\mu$ . They called  $Mi, Mi'$  ( $i = 2, 4, 6, 8, 9$ ),  $M_0$  ( $e = 0$ ) with eccentricities 0.2, 0.4, 0.6, 0.8, and 0.9, respectively; and they started with  $v_0 = 0(Mi)$  and  $v_0 = \pi(Mi')$ .

The numerical results of these families for the first member of each one, are shown in Table I.

The second group includes 20 families of periodic orbits, which they found by

TABLE I

	$x_{01}$	$x_{05}$	$x_{06}$	$x_1$	$x_5$	$x_6$	S	$k_1$	$k_2$	$k_3$	M
$M_0$	1.0595	-1.5083	0.9292	-0.3239	0.9086	1.6322	9.6E+04	-002	-003	010	0.01
$M_2$	1.0833	-1.4613	0.9481	1.0776	-1.4973	-0.9795	0.1E+12	-003	200	060	0.02
$M_4$	1.0904	-1.5007	0.9159	0.0774	-1.5089	-0.9825	-0.2E+12	300	100	-003	0.02
$M_6$	1.1279	-1.5610	0.8749	1.0904	-1.7340	-1.0217	-0.2E+13	500	070	-004	0.03
$M_8$	1.2308	-1.7720	0.7398	1.1022	-2.1638	-1.0495	-0.3E+13	600	20	-020	0.04
$M_9$	1.7579	-2.2200	0.5862	1.1112	-2.8482	-1.4232	-0.2E+14	300	-400	-300	0.07
$M'_2$	1.0900	-1.4787	1.0032	1.0982	-1.4370	-0.9631	0.1E+12	-003	200	70	0.03
$M'_4$	1.0892	-1.5625	1.0178	1.1079	-1.4696	-0.9320	-0.2E+12	300	100	-030	0.03
$M'_6$	1.0985	-1.7240	1.0637	1.1469	-1.5349	-0.8866	-0.2E+13	500	80	-004	0.04
$M'_8$	1.1140	-2.1467	1.2535	1.3246	-1.7222	-0.7780	-0.3E+13	500	70	-010	0.07
$M'_9$	1.1099	-2.5098	1.8222	2.0285	-2.3489	-0.6079	0.5E+13	-600	3	40	0.11

TABLE II

	$x_{01}$	$x_{05}$	$x_{06}$	$x_1$	$x_5$	$x_6$	S	$k_1$	$k_2$	$k_3$	M
$E_1$	1.1480	-1.4092	0.9714	1.1241	-1.4671	-1.0498	5.5E+10	-2.9	130	58	0.1
$E_2$	1.1718	-1.4383	0.9373	1.1268	-1.4986	-1.0461	4.4E+09	-3.4	098	31	0.2
$E_3$	1.1785	-1.4776	0.8959	1.1128	-1.5310	-1.0231	2.9E+08	-3.7	72	15	0.3
$E_4$	1.1775	-1.5183	0.8539	1.0913	-1.5605	-0.9927	2.5E+07	-3.8	52	8.1	0.4
$E_5$	1.1726	-1.5590	0.8183	1.0659	-1.5872	-0.9591	6.1E+06	-3.8	37	7.3	0.5
$E_6$	1.1650	-1.5994	0.7746	1.0382	-1.6115	-0.9239	2.2E+06	-3.8	26	8.1	0.6
$E_7$	1.1558	-1.6395	0.7381	1.0091	-1.6343	-0.8883	6.6E+05	-3.7	17	8.5	0.7
$E_8$	1.1454	-1.5794	0.7040	0.9792	-1.6558	-0.8530	0.1E+06	-4	10	8	0.8
$E_9$	1.1340	-1.7194	0.6720	0.9490	-1.6767	-0.8152	0.1E+05	-4	4	6	0.9
$E_{10}$	1.1245	-1.7514	0.6480	0.9247	-1.6931	-0.7911	0.2E+03	-4	-0.4	3	0.98
$E'_1$	1.1241	-1.4675	1.0498	1.1480	-1.4092	-0.9714	5.5E+10	-2.9	130	58	0.1
$E'_2$	1.1268	-1.4986	1.0461	1.1718	-1.4383	-0.9373	4.4E+09	-3.3	98	31	0.2
$E'_3$	1.1128	-1.5310	1.0231	1.1785	-1.4776	-0.8959	2.9E+08	-3.7	72	15	0.3
$E'_4$	1.0913	-1.5605	0.9927	1.1776	-1.5183	-0.8539	2.5E+07	-3.8	52	8.1	0.4
$E'_5$	1.0659	-1.5872	0.9591	1.1726	-1.5590	-0.8133	6.1E+06	-3.8	37	7.3	0.5
$E'_6$	1.0382	-1.6115	0.9239	1.1650	-1.5994	-0.7746	2.2E+06	-3.8	26	8.1	0.6
$E'_7$	1.0091	-1.6343	0.8883	1.1558	-1.6395	-0.7381	6.6E+05	-3.8	17	8.5	0.7
$E'_8$	0.9792	-1.6558	0.8530	1.1454	-1.6794	-0.7040	0.1E+06	-4	10	8	0.8
$E'_9$	0.9490	-1.6767	0.8182	1.1340	-1.7194	-0.6720	0.1E+05	-4	4	6	0.9
$E'_{10}$	0.9247	-1.6931	0.7911	1.1245	-1.7514	-0.6480	0.2E+03	-4	-0.4	3	0.98

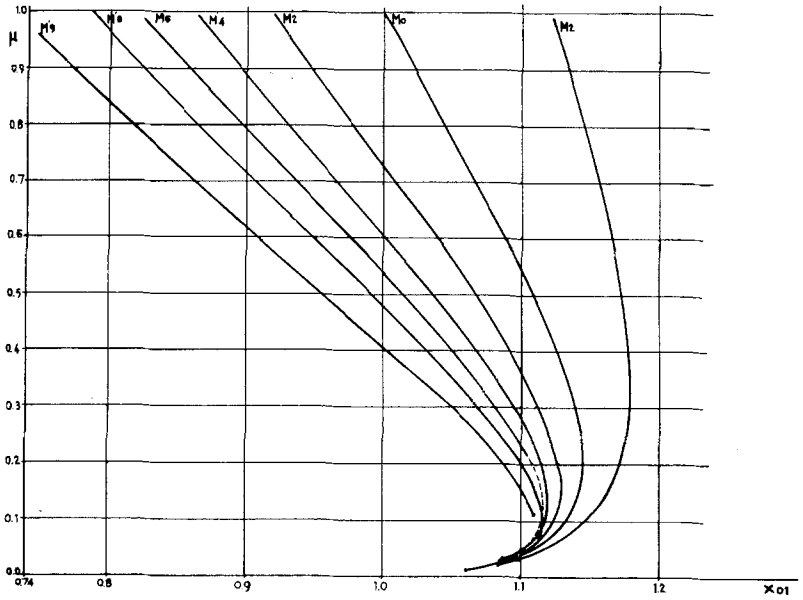


Fig. 1. Characteristic curves of the  $M'$  families.

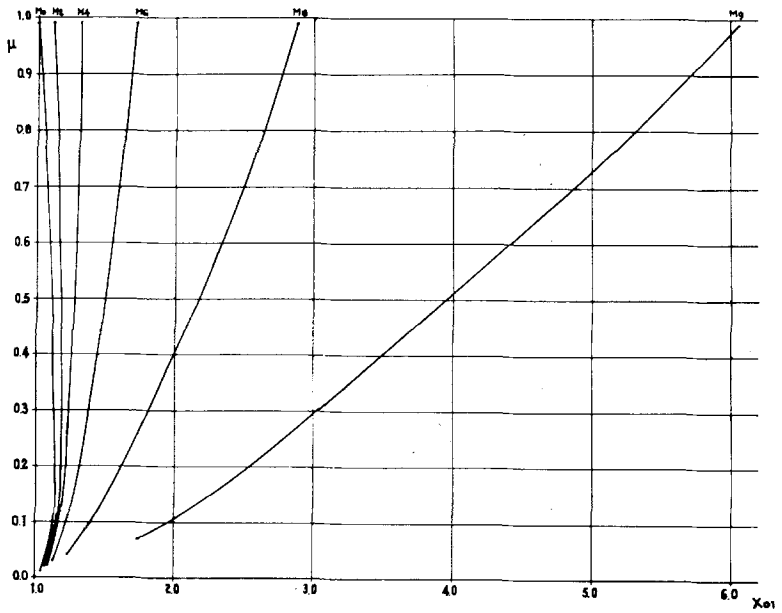


Fig. 2. Characteristic curves of the  $M$  families.



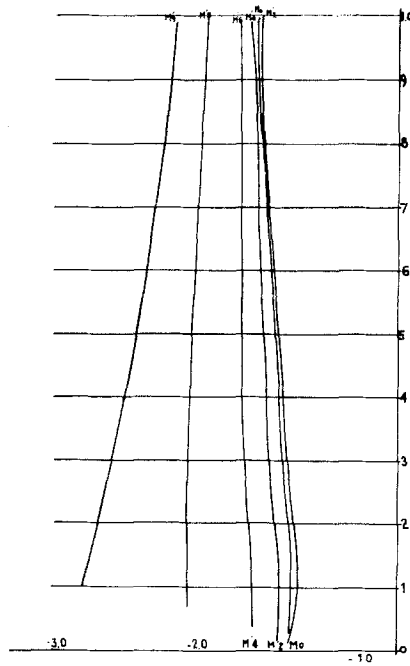


Fig. 3. Change of  $x_{05}$  (projection of the velocity on the  $Ox_1$ -axis) as a function of the mass rate  $\mu$  ( $M'$  families).

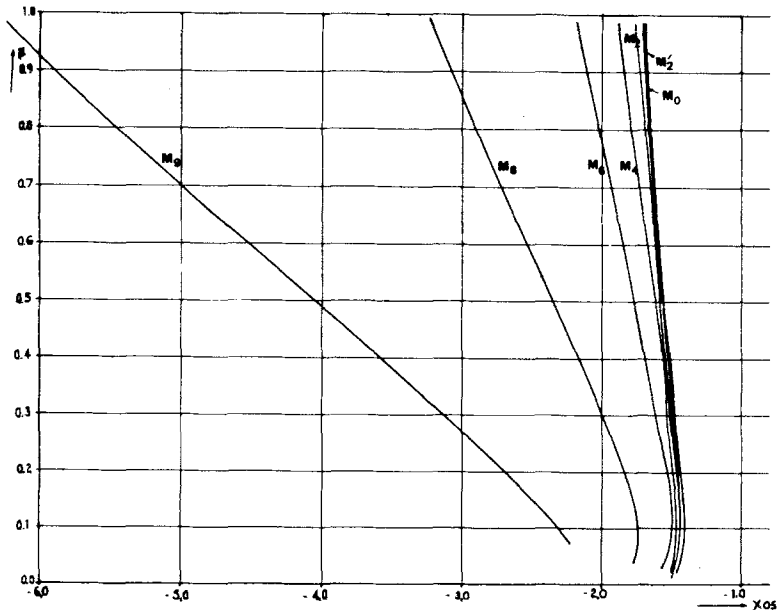


Fig. 4. Change of  $x_{05}$  (projection of the velocity on the  $Ox_1$ -axis) as a function of the mass rate  $\mu$  ( $M$  families).

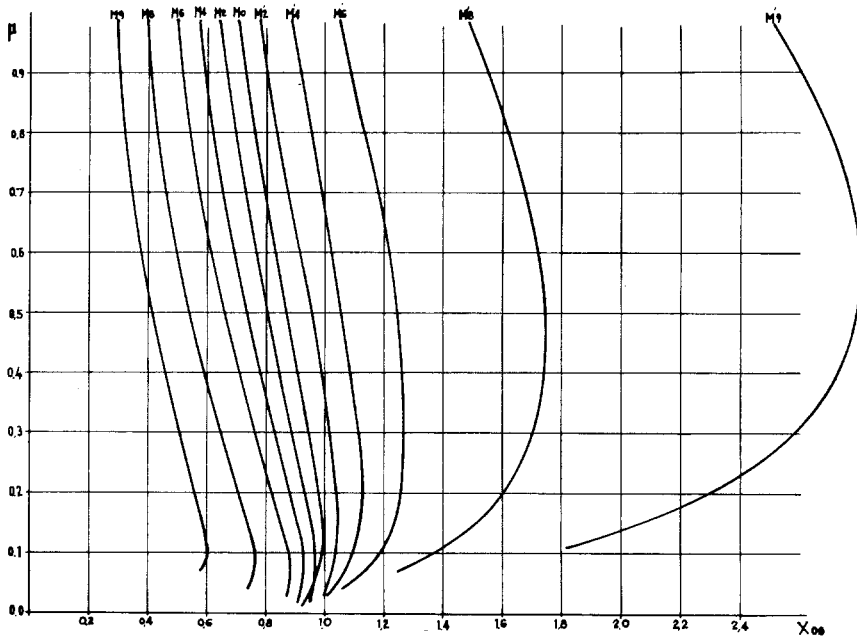


Fig. 5. Change of  $x_{06}$  (projection of the velocity on the  $Ox_3$ -axis) as a function of the mass rate  $\mu$ .

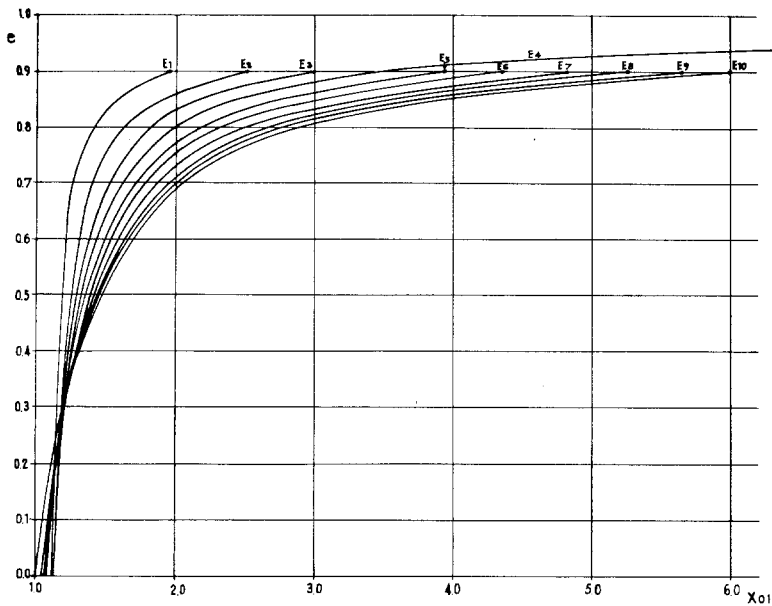


Fig. 6. Change of the  $x_{01}$  ( $X$ -coordinate) as a function of the eccentricity  $e$ .

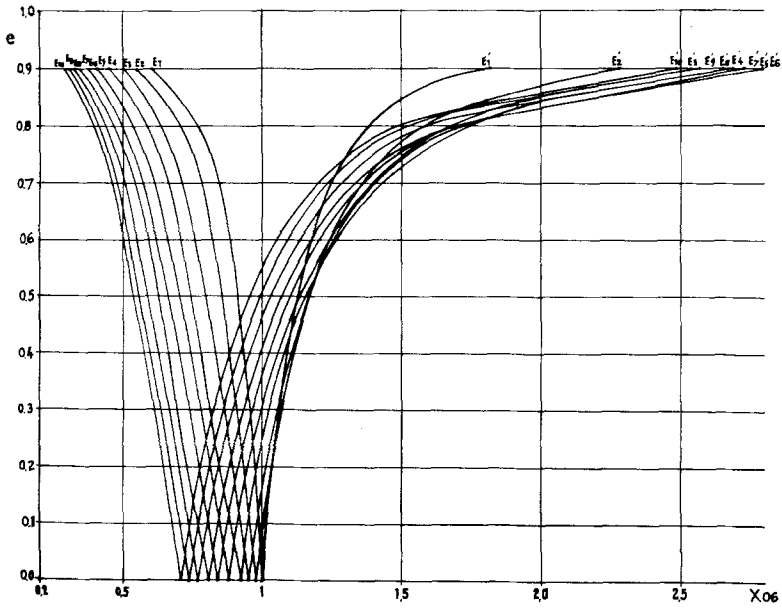


Fig. 7. Change of  $x_{06}$  (projection of the velocity on the  $Ox_3$ -axis) as a function of the eccentricity  $e$ .

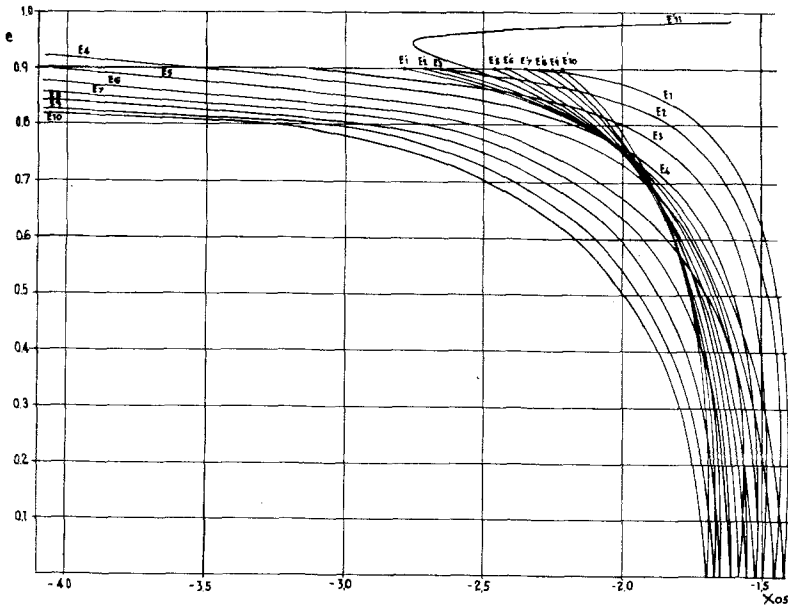


Fig. 8. Change of  $x_{05}$  (projection of the velocity on the  $Ox_2$ -axis) as a function of the eccentricity  $e$ .

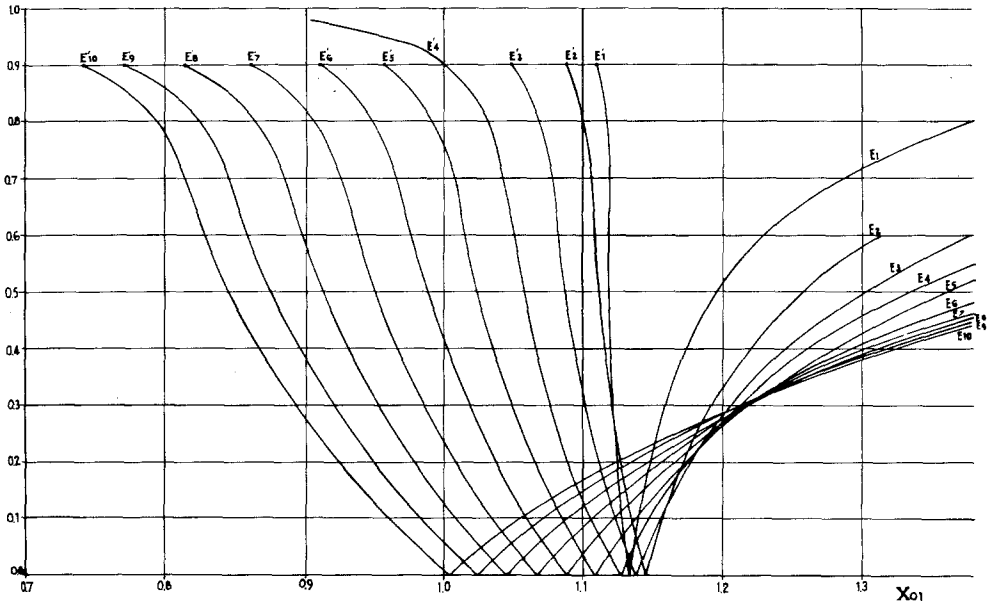


Fig. 9. Change of the  $x_{01}$  ( $X$ -coordinate) as a function of the eccentricity  $e$ .

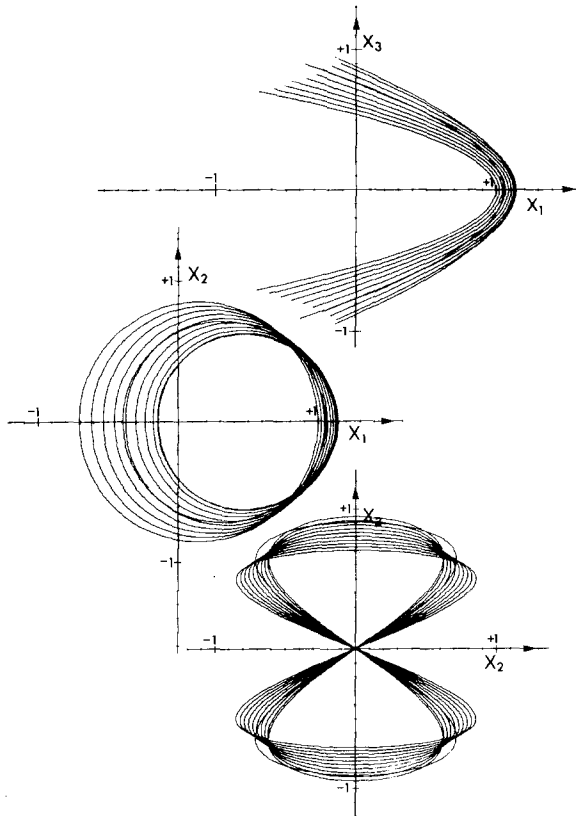


Fig. 10. Projections of 10 orbits of the  $M_0$  family on the  $Ox_1x_3$ ,  $Ox_1x_2$ , and  $Ox_2x_3$  planes.

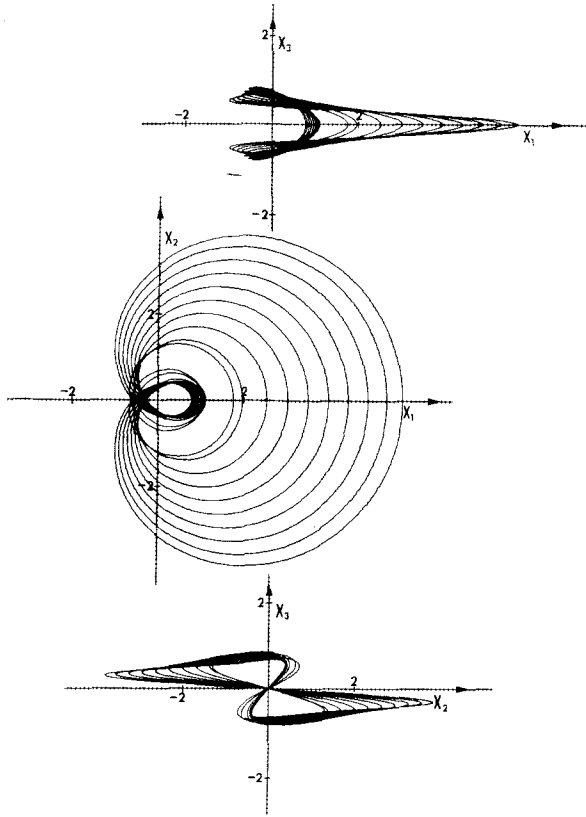


Fig. 11. Projections of 10 orbits of the  $M_9$  family on the  $Ox_1x_3$ ,  $Ox_1x_2$ , and  $Ox_2x_3$  planes.

changing the eccentricity  $e$  and are called  $E_i$  and  $E'_i$ ,  $i = 1, 2, 3, 4, 5, 6, 7, 8, 9, 10$ . Of each one of these families beginning for values of  $\mu$ , 0.1, 0.2, 0.3, ..., 0.9, 0.98, respectively, and  $e = 0$ .

The numerical results of the  $E$  families for the member of each family, which has  $e = 0.2$  are shown in Table II.

Each one of these tables contains.

- (1) The initial conditions  $x_{01}$ ,  $x_{05}$ ,  $x_{06}$  of each calculated orbit.
- (2) The values  $x_1$ ,  $x_5$ ,  $x_6$  at the end of the half-period.
- (3) The quantity  $S = q^3 + r^2$  defines in which half-space of stability or instability the orbit is located. If  $S > 0$  the orbit is unstable, if  $S < 0$  and  $|ki| \leq 2$ ,  $i = 1, 2, 3$  the orbit is stable, and if the  $|ki| > 2$ , is unstable.
- (4) The quantities  $k_1$ ,  $k_2$ ,  $k_3$  (stability indices).
- (5) The quantities  $E$  or  $M$ , which define the eccentricity  $e$  and the mass ratio  $\mu$ , respectively.

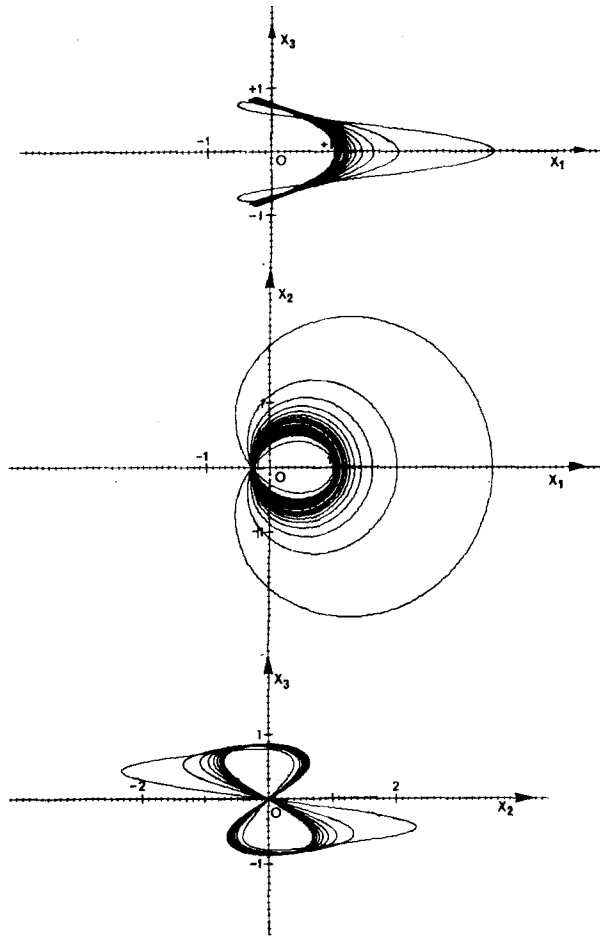


Fig. 12. Projections of 10 orbits of the  $E_4$  family on the  $Ox_1x_3$ ,  $Ox_1x_2$ , and  $Ox_2x_3$  planes.

### 5. Concluding Remarks

As it appears in the figures of the orbits  $M_i$  and  $M_i'$ , we have symmetry of the orbits of these families for  $i = 2, 4, 6, 8, 9$ , with respect to the plane  $ox_1x_3$ . Actually, we observe that for the same  $\mu$  and  $e$  the orbits  $M$  and  $M'$  have the following relations  $x_{01} = x'_1$ ,  $x_{05} = x'_5$ ,  $x_{06} = x'_6$  (where  $x_{01}, x_{05}, x_{06}$  the initial conditions of the orbits  $M$  and  $x'_1, x'_5, x'_6$  the conditions of the orbits  $M'$  at the end of the half-period).

The families  $E_4$  and  $E'_4$  have been studied more than the others. Figure 6 shows the changes of  $x_{01}$  in function of  $e$ .

We observe that for small values of  $e$  the changes of  $x_{01}$  are small, whereas for values of  $e > 0.91$  the changes of  $x_{01}$  are greater than in the first case. For that reason in order to find the next orbit of the family we should give to  $e$  very small variations.

If we compare the numerical of the  $E$  and  $E'$  orbits, for the same  $\mu$  and  $e$ , the time

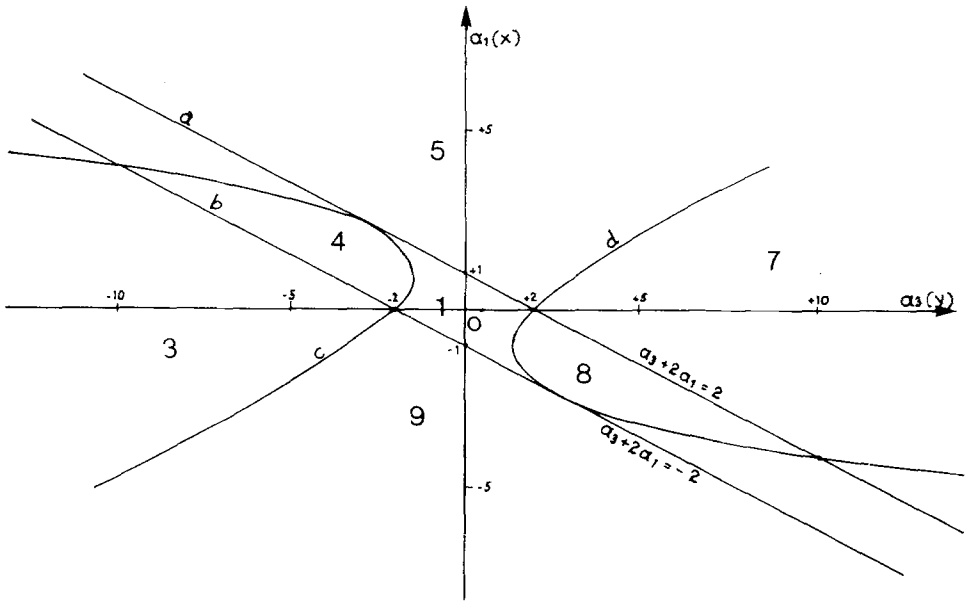


Fig. 13. Intersection of stability-instability regions by the  $OXY$ -plane.

$v$  and  $2\pi - v$ , respectively, we shall observe that  $x_1 = x'_1$ ,  $x_2 = -x'_2$ , and  $x_3 = x'_3$ , which means that the two orbits are symmetrical with respect to the plane  $Ox_1x_3$ .

Figures 2, 3, 4, and 5 show the characteristic curves of the families  $M$ .

Figures 6, 7, 8, and 9 show the characteristic curves of the families  $E$ .

Figures 10, 11, and 12 show the morphological evolution of the orbits of the various families.

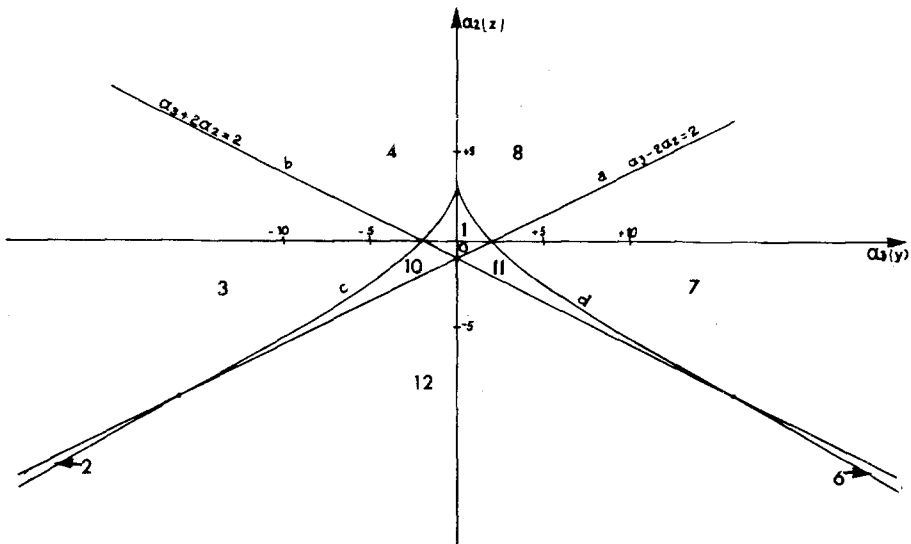


Fig. 14. Intersection of stability-instability regions by the  $OYZ$ -plane.

The families of the periodic orbits have two parameters (the eccentricity  $e$  of the primaries and the mass ratio  $\mu$ ). For this reason the new families of periodic orbits have been found, through variation of either the mass ratio  $\mu$  or the eccentricity  $e$ . Eleven families of the first kind and twenty of the second were studied.

Orbits of the circular problem were considered to be the starting points. These orbits are found on the surface of a cylinder. The intersection of the cylinder with the plane  $Ox_1x_2$  is a circle or an ellipse. These orbits are also symmetric with respect to  $Ox_1$ -axis as well as with respect to  $Ox_1x_2$ -plane.

In the elliptical case the orbits are also found on the surface of a cylinder, which is perpendicular to the plane  $Ox_1x_2$  and forms a loop. But in no case orbits with double symmetry found. These orbits can be distinguished in two kinds: orbits with starting point the primaries in the shorter possible distance and orbits with starting point the primaries in the longest distance. These two kinds of orbits were found in the present study to be symmetric to each other about the plane  $Ox_1x_3$ .

### Acknowledgement

The author would like to thank his friend Dr M. Zikides for helpful suggestions during the course of the investigation.

### References

- Bray, T. A. and Goudas, G. L.: 1966, *Three-Dimensional Periodic Oscillations about  $L_1$ ,  $L_2$ , and  $L_3$* , Boeing Scientific Research Laboratories, No. 467.
- Bray, T. A. and Goudas, C. L.: 1967, *Astro. J.* **72**, 202.
- Broucke, R. A.: 1969, *Periodic Orbits in the Elliptic Restricted Three-Body Problem*, Jet Propulsion Laboratory Technical Report 32-1360.
- Hunter, R. B.: 1967, *Monthly Notices Roy. Astron. Soc.* **136**, 245.
- Katsiaris, G. A.: 1972, in B. D. Tapley and V. Szebehely (eds.), *Recent Advances in Dynamical Astronomy*, D. Reidel Publ. Co., Dordrecht, Holland, p. 118.
- Kopal, Z. and Lyttleton, R. A.: 1963, *Icarus* **1**, 230.
- Macris, G., Katsiaris, G. A., and Goudas, C. L.: 1975, *Astrophys. Space Sci.* **33**, 333.